Original Article | Genitourinary Imaging

eISSN 2005-8330
https://doi.org/10.3348/kjr.2023.0760
Korean J Radiol 2024;25(1):43-54

Korean Journal of Radiology
KJR

Differentiating Uterine Sarcoma From Atypical Leiomyoma on Preoperative Magnetic Resonance Imaging Using Logistic Regression Classifier: Added Value of Diffusion-Weighted Imaging-Based Quantitative Parameters

Hokun Kim[1], Sung Eun Rha[1], Yu Ri Shin[1,2], Eu Hyun Kim[3], Soo Youn Park[3], Su-Lim Lee[4], Ahwon Lee[5], Mee-Ran Kim[6]

[1]Department of Radiology, Seoul St. Mary's Hospital, College of Medicine, The Catholic University of Korea, Seoul, Republic of Korea
[2]Department of Radiology, Incheon St. Mary's Hospital, College of Medicine, The Catholic University of Korea, Incheon, Republic of Korea
[3]Department of Radiology, St. Vincent's Hospital, College of Medicine, The Catholic University of Korea, Suwon, Republic of Korea
[4]Department of Radiology, Uijeongbu St. Mary's Hospital, College of Medicine, The Catholic University of Korea, Uijeongbu, Republic of Korea
[5]Department of Hospital Pathology, Seoul St. Mary's Hospital, College of Medicine, The Catholic University of Korea, Seoul, Republic of Korea
[6]Department of Obstetrics and Gynecology, Seoul St. Mary's Hospital, College of Medicine, The Catholic University of Korea, Seoul, Republic of Korea

Objective: To evaluate the added value of diffusion-weighted imaging (DWI)-based quantitative parameters to distinguish uterine sarcomas from atypical leiomyomas on preoperative magnetic resonance imaging (MRI).

Materials and Methods: A total of 138 patients (age, 43.7 ± 10.3 years) with uterine sarcoma (n = 44) and atypical leiomyoma (n = 94) were retrospectively collected from four institutions. The cohort was randomly divided into training (84/138, 60.0%) and validation (54/138, 40.0%) sets. Two independent readers evaluated six qualitative MRI features and two DWI-based quantitative parameters for each index tumor. Multivariable logistic regression was used to identify the relevant qualitative MRI features. Diagnostic classifiers based on qualitative MRI features alone and in combination with DWI-based quantitative parameters were developed using a logistic regression algorithm. The diagnostic performance of the classifiers was evaluated using a cross-table analysis and calculation of the area under the receiver operating characteristic curve (AUC).

Results: Mean apparent diffusion coefficient value of uterine sarcoma was lower than that of atypical leiomyoma (mean ± standard deviation, 0.94 ± 0.30 10^{-3} mm^2/s vs. 1.23 ± 0.25 10^{-3} mm^2/s; $P < 0.001$), and the relative contrast ratio was higher in the uterine sarcoma (8.16 ± 2.94 vs. 4.19 ± 2.66; $P < 0.001$). Selected qualitative MRI features included ill-defined margin (adjusted odds ratio [aOR], 17.9; 95% confidence interval [CI], 1.41–503, $P = 0.040$), intratumoral hemorrhage (aOR, 27.3; 95% CI, 3.74–596, $P = 0.006$), and absence of T2 dark area (aOR, 83.5; 95% CI, 12.4–1916, $P < 0.001$). The classifier that combined qualitative MRI features and DWI-based quantitative parameters showed significantly better performance than without DWI-based parameters in the validation set (AUC, 0.92 vs. 0.78; $P < 0.001$).

Conclusion: The addition of DWI-based quantitative parameters to qualitative MRI features improved the diagnostic performance of the logistic regression classifier in differentiating uterine sarcomas from atypical leiomyomas on preoperative MRI.

Keywords: Uterus; Uterine sarcoma; Uterine leiomyoma; Magnetic resonance imaging; Diagnosis; Diffusion-weighted imaging; Apparent diffusion coefficient value; Relative contrast ratio

INTRODUCTION

Leiomyomas are common benign neoplasms of the uterus that affect approximately 40% of reproductive-age women [1,2]. Although most patients with leiomyomas are asymptomatic, one-third may experience symptoms such

Received: August 19, 2023 **Revised:** October 17, 2023 **Accepted:** October 24, 2023
Corresponding author: Sung Eun Rha, MD, PhD, Department of Radiology, Seoul St. Mary's Hospital, College of Medicine, The Catholic University of Korea, 222 Banpo-daero, Seocho-gu, Seoul 06591, Republic of Korea
• E-mail: serha@catholic.ac.kr

as abdominal pain, palpable mass, or vaginal bleeding [3]. Meanwhile, uterine sarcomas are rare tumors, comprising 2%–7% of uterine malignancies, and often present with clinical manifestations similar to leiomyomas, which pose challenges for accurate differentiation [4,5]. This diverse group of tumors, originating from the mesenchymal layer of the uterus, includes leiomyosarcomas, the most common subtype, endometrial stromal sarcomas (ESS), adenosarcomas, and undifferentiated sarcomas [6]. Despite their similar clinical presentation, leiomyomas and uterine sarcomas have different clinical courses. Uterine sarcomas are associated with a poor prognosis, aggressive growth, and high metastatic potential [7]. The accurate preoperative diagnosis of uterine sarcoma is crucial to ensure appropriate surgical resection and prevent the use of uterus-preserving treatments, such as gonadotropin-releasing hormone analogs, uterine arterial embolization, and focused ultrasound surgery, which are considered inappropriate in the presence of sarcoma. In a December 2017 report, the U.S. Food and Drug Administration revealed that uterine sarcomas were found in approximately 1 in 225–580 women undergoing surgery for uterine fibroids, along with a cautionary statement regarding the potential for intraperitoneal morcellation-associated dissemination [8].

Magnetic resonance imaging (MRI) of the pelvis is one of the most important diagnostic modalities for the preoperative evaluation of uterine tumors. Typical leiomyomas are easily recognized on MRI by their classic appearance as well-circumscribed masses with homogeneously low signal intensity (SI) on both T2-weighted and diffusion-weighted images (T2WI and diffusion-weighted imaging [DWI], respectively) [9-11]. However, leiomyomas can occasionally present with degenerative changes or cellular histological subtypes, resulting in atypical imaging findings such as heterogeneous high SI on T2WI and/or intratumoral hemorrhage, closely similar to uterine sarcomas [12]. These are commonly referred to as "atypical leiomyomas." Several studies have been conducted to differentiate uterine sarcomas from leiomyomas using preoperative MRI [11-27]. These studies mainly analyzed the imaging features on conventional T2WI and contrast-enhanced images, as well as DWI and apparent diffusion coefficient (ADC) maps. There is a consensus that the lower the ADC value, the greater the likelihood of malignancy in the diagnosis of uterine sarcoma. However, only a few studies have focused on distinguishing between leiomyomas with atypical imaging features (e.g., atypical leiomyoma) and uterine sarcomas [11,12,15,23,25]. Furthermore, most studies either excluded ESS or included only a limited number of ESS cases despite ESS being a significant differential diagnosis for atypical leiomyomas. This study aimed to evaluate the diagnostic value of DWI-based quantitative parameters when added to qualitative MRI features to distinguish uterine sarcoma from atypical leiomyoma on preoperative MRI using a machine learning classifier.

MATERIALS AND METHODS

Patient Selection

This study was approved by the Catholic Medical Center Institutional Review Board and the requirement of informed consent was waived (IRB No. XC18REDI0064). Two cohorts of patients, as follows, were retrospectively analyzed: one with uterine sarcoma and the other with atypical leiomyoma. For the uterine sarcoma group, the pathology databases of four institutions (Seoul St. Mary's Hospital, Incheon St. Mary's Hospital, St. Vincent's Hospital, and Uijeongbu St. Mary's Hospital) were searched from January 2010 to December 2021. The atypical leiomyoma group was identified from the pelvic MRI radiological report database of Seoul St. Mary's Hospital between January 2013 and December 2020. We used specific descriptions and diagnostic impressions commonly used by radiologists when suspective of the presence of uterine tumors that do not present with typical imaging findings of uterine leiomyomas (e.g., atypical/unusual uterine/myometrial mass, cellular leiomyoma/fibroid, or uterine sarcoma/leiomyosarcoma/ESS). The inclusion criteria were the following: 1) pathological confirmation by surgical resection and 2) the presence of a preoperative multiparametric pelvic MRI with DWI. Finally, all identified patients were randomly assigned to the training (60%) and validation (40%) sets for diagnostic classifier development. Finally, 138 patients (mean age, 43.7 ± 10.3 years) with uterine sarcoma (n = 44) and atypical leiomyoma (n = 94) were included. There were 35 patients with uterine sarcoma at Seoul St. Mary's Hospital, 5 at Incheon St. Mary's Hospital, 3 at St. Vincent's Hospital, and 1 at Uijeongbu St. Mary's Hospital. The cohort was randomly divided into training (84/138, 60.0%) and validation (54/138, 40.0%) sets. The details are shown in Figure 1.

Magnetic Resonance Imaging Technique

Various MRI scanners and scanning protocols were used owing to the retrospective, multi-institutional nature of the study. A total of 120 patients underwent MRI using a

https://doi.org/10.3348/kjr.2023.0760

Korean Journal of Radiology
KJR

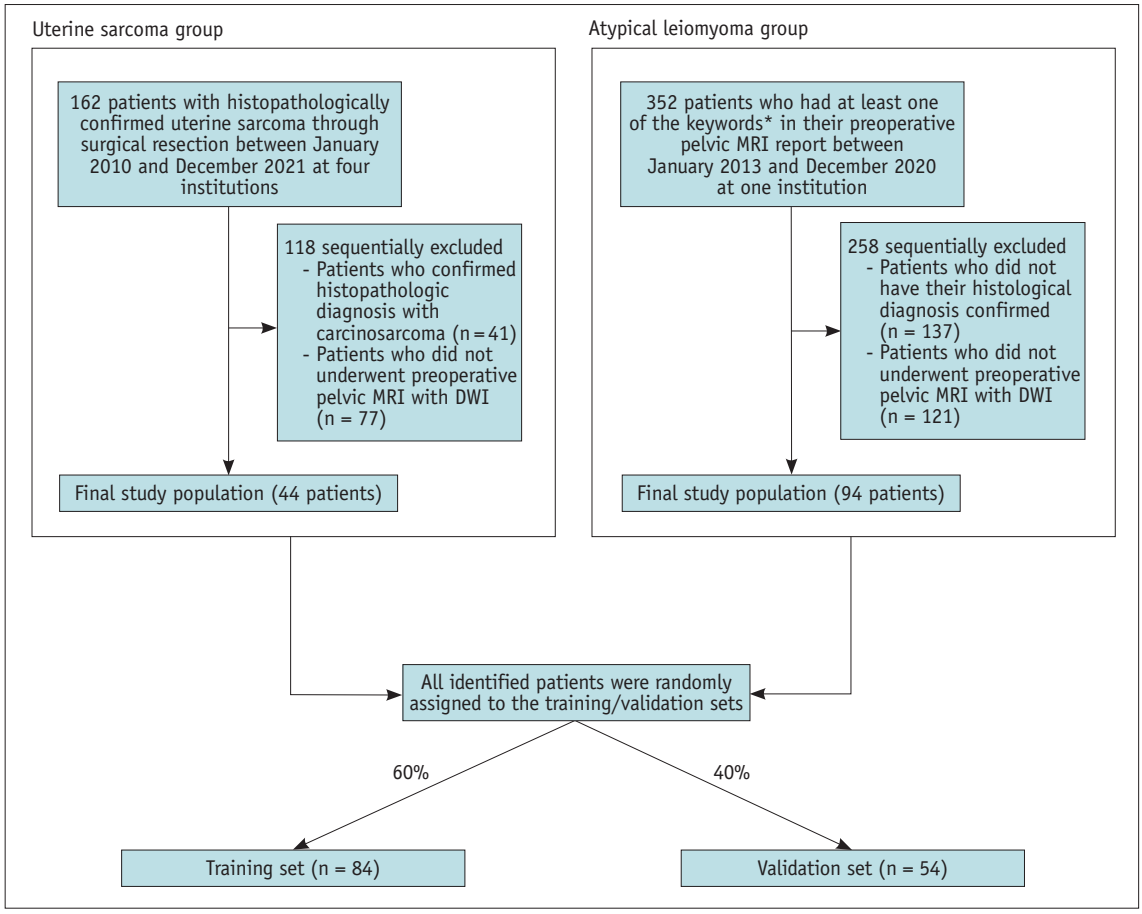

Fig. 1. Flow diagram of the study population. *Keywords: atypical/unusual uterine/myometrial mass, cellular leiomyoma/fibroid, uterine sarcoma/leiomyosarcoma/endometrial stromal sarcoma. MRI = magnetic resonance imaging, DWI = diffusion-weighted imaging

3.0-T system, while 18 patients were examined with a 1.5-T system. All patients were examined in the supine position, and a phased-array coil was used to perform body scans. All imaging protocols included at least axial and sagittal T2WI fast spin-echo images, axial T1-weighted images (T1WI), fat-suppressed T1WI after intravenous gadolinium injection (0.1 mmol/kg body weight and a rate of 2–3 mL/s), and DWI. Axial or oblique axial DWI was performed using single-shot echo-planar imaging with fat suppression. ADC maps were generated from isotropic DWI with b-values of 0 and 800 (n = 6) or 1000 (n = 132) s/mm^2 by calculating the slope of the logarithmic decay curve for SI against the b-value. Supplementary Table 1 shows the detailed imaging protocol for the most frequently used scanner (3.0-T Magnetom Verio; Siemens Healthineers).

Image Analysis

Two board-certified radiologists (H. K. and S. E. R., with 7 and 29 years of gynecologic imaging experience, respectively), who were blinded to clinical data and histopathological results, independently interpreted the magnetic resonance images on a picture archiving and communication system workstation monitor.

Two readers evaluated the following basic tumor characteristics and qualitative MRI features of the index tumor: 1) size; 2) shape (round/oval vs. irregular/lobulated); 3) margin (well-circumscribed vs. ill-defined); 4) presence of intratumoral hemorrhage, defined as a focal area of high SI on fat-suppressed T1WI; 5) presence of intratumoral cystic areas (SI equal to that of urine) on T2WI; 6) absence of T2 dark area, defined as the absence of intratumoral low SI solid portion lower than the SI of gluteal muscle on T2WI [11]; and 7) presence of necrosis manifesting as central irregular unenhanced area(s). For patients with more than one myometrial mass (n = 70), the index tumor was defined as the largest lesion that did not correspond to the MRI features of a typical leiomyoma and was correlated with histopathological findings.

 https://doi.org/10.3348/kjr.2023.0760

To measure DWI-based quantitative parameters, each reader manually delineated a singular circular region of interest (ROI) on the solid component of the tumor within the ADC maps and high b-value DWI images, while referencing T2WI and contrast-enhanced T1WI. The ROI was defined as the representative slice within the ADC map exhibiting the most pronounced diffusion restriction (the darkest region on the ADC map, corresponding to the brightest area on high-b-value DWI images, and the enhanced solid region on contrast-enhanced imaging). Careful attention was paid to avoid necrotic and cystic portions of the tumor. Subsequently, the delineated ROI was duplicated and positioned on the corresponding high b-value DWI slice. Similarly, a circular ROI was traced on adjacent hip or back muscles on an identical high b-value DWI slice to compute the relative contrast ratio (RCR) of the tumor. The RCR was calculated as follows: RCR = SI (mass on high b-value DWI)/SI (muscle on high b-value DWI) [28]. Each reader repeated the measurements twice, and the average value was used in the analysis. Representative cases of uterine sarcoma and atypical leiomyoma with DWI-based quantitative parameter measurements are shown in Figures 2 and 3.

Diagnostic Classifier Development

Any disagreements in the qualitative MRI features obtained between the readers were resolved by consensus. DWI-based quantitative parameters measured by a more experienced radiologist (S. E. R., reader 2) were used for the development of the diagnostic classifier. In the training phase, univariable and multivariable logistic regression analyses were used to identify relevant MRI features to differentiate uterine sarcomas from atypical leiomyomas. MRI features with $P < 0.05$ in the univariable analysis were included in the multivariable analysis. For multivariable logistic regression

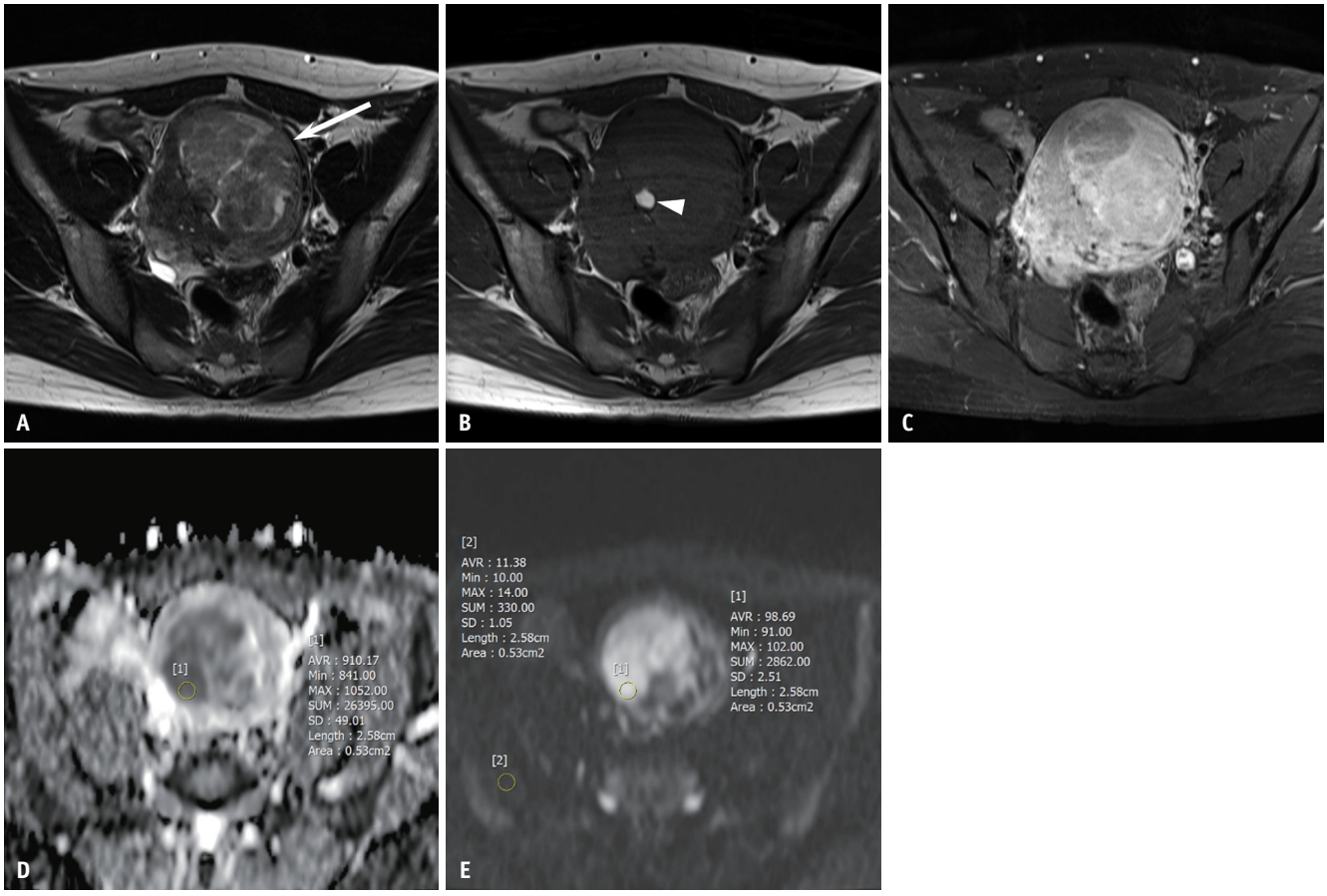

Fig. 2. Uterine leiomyosarcoma in a 42-year-old female. **A:** Axial T2WI reveals an oval, well-circumscribed, slightly hyperintense myometrial tumor (arrow). No intratumoral low SI solid portion with a whorled appearance is observed on T2WI. **B:** Axial T1WI shows a small area of intratumoral hemorrhage (arrowhead). **C:** Axial contrast-enhanced T1WI shows heterogeneous enhancement of the tumor. The mean ADC value of the tumor is 0.91 x 10^{-3} mm^2/s **(D)**, and the RCR is 8.66 (98.7/11.4) on high b-value DWI (b = 1000 s/mm^2) **(E)**. T2WI = T2-weighted image, SI = signal intensity, T1WI = T1-weighted image, ADC = apparent diffusion coefficient, RCR = relative contrast ratio, DWI = diffusion-weighted imaging, AVR = average, Min = minimum, MAX = maximum, SD = standard deviation

https://doi.org/10.3348/kjr.2023.0760

Korean Journal of Radiology
KJR

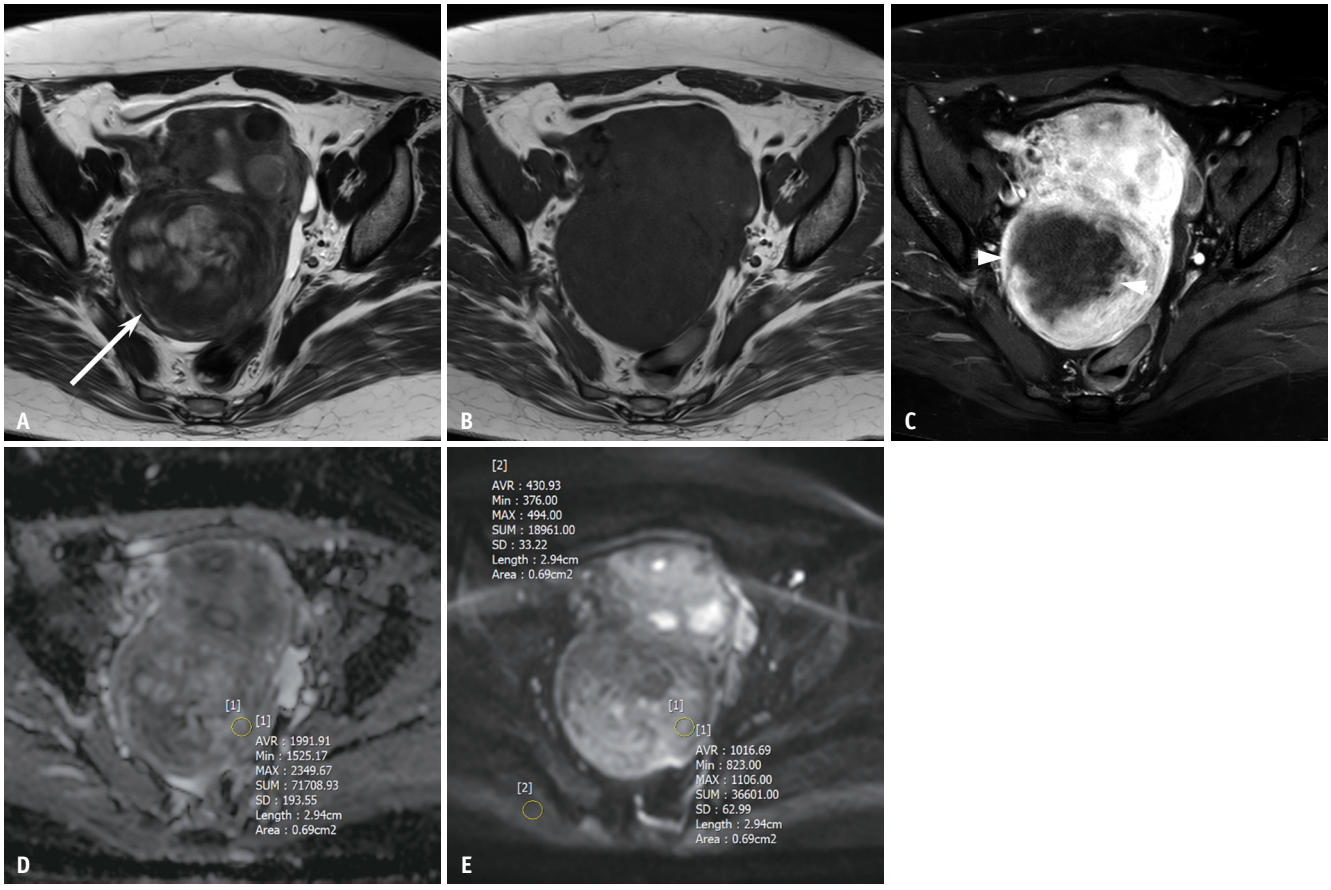

Fig. 3. Atypical leiomyoma in a 51-year-old female. **A:** Axial T2WI shows an oval, well-circumscribed, hypointense myometrial tumor (arrow) with central heterogeneous high SI areas. **B:** No evidence of intratumoral hemorrhage is observed on axial T1WI. **C:** Axial contrast-enhanced T1WI shows a large central unenhanced area (arrowheads). The mean ADC value of the solid portion of the tumor is 1.99 x 10^{-3} mm^2/s **(D)**, and the RCR is 2.36 (1017/431) on high b-value DWI (b = 1000 s/mm^2) **(E)**. T2WI = T2-weighted image, SI = signal intensity, T1WI = T1-weighted image, ADC = apparent diffusion coefficient, RCR = relative contrast ratio, DWI = diffusion-weighted imaging, AVR = average, Min = minimum, MAX = maximum, SD = standard deviation

analysis, qualitative MRI features with $P < 0.05$ were chosen. Three diagnostic classifiers were then built using a logistic regression algorithm from the caret R package (6.0-92, https://github.com/topepo/caret/), and qualitative MRI features were collected from the multivariable logistic regression analysis alone, combining the qualitative MRI features and mean ADC values, and combining the qualitative MRI features and both mean ADC values and RCR. Three repeated 10-fold cross-validations were performed for each classifier during the training process, and a grid search technique was used for hyperparameter tuning.

Statistical Analysis

Categorical variables are shown as numbers with frequencies and were compared using χ^2 or Fisher's exact tests. Continuous variables are summarized as means with standard deviations and were compared using Mann–Whitney U or Student's *t*-tests. Odds ratios are presented as 95% confidence intervals (CIs). The cutoff points for the ADC value, RCR, and all diagnostic classifiers were determined using the receiver operating characteristic (ROC) curve with the maximum Youden index in the training set. Subsequently, the diagnostic performance of the generated diagnostic classifiers was compared using metrics such as accuracy, sensitivity, specificity, and area under the ROC curve (AUC). Delong's test was used to compare two AUCs. Kappa values and intraclass correlation coefficients (ICCs) were calculated to assess the interobserver agreement between the two readers. A kappa value and ICC of 0.00–0.20, 0.21–0.40, 0.41–0.60, 0.61–0.80, and 0.81–1.00 indicated a slight agreement, fair agreement, moderate agreement, substantial agreement, and almost perfect agreement, respectively. Statistical analyses were performed with R (version 4.2.1; R Foundation for Statistical Computing). A *P*-value < 0.05 was

 https://doi.org/10.3348/kjr.2023.0760

considered a statistically significant difference.

RESULTS

Patient Characteristics

The clinical characteristics of the two subgroups, uterine sarcoma and atypical leiomyoma and the training and validation sets are shown in Table 1. Patients with uterine sarcomas were significantly older than those with atypical leiomyomas. The mean interval between MRI and surgery was 41.2 days (range, 0–191 days), and the interval was significantly shorter in patients diagnosed with uterine sarcoma. The maximal diameters of the uterine sarcomas and atypical leiomyomas were not significantly different. The two most prevalent pathological subtypes of uterine sarcoma included in this study were leiomyosarcoma (n = 21) and ESS (n = 19). The training set included 27 patients with uterine sarcomas and 57 patients with atypical leiomyomas. Thirty-seven patients in the validation set had atypical leiomyoma and 17 had uterine sarcoma. A total of 65.9% (29/44) of uterine sarcomas presented as solitary masses, while 41.5% (39/94) of atypical leiomyomas presented as single masses. No significant differences in clinical characteristics were observed between the training and validation sets, except for the mean interval between MRI and surgery.

Image Analysis

Table 2 shows the detailed results of the image analysis for both the readers' qualitative and quantitative MRI features. All six qualitative MRI features were significantly different between uterine sarcoma and atypical leiomyoma according to reader 1, but not in the margin and cystic areas on T2WI according to reader 2 (P = 0.078 and P = 0.143, respectively). The mean ROI sizes measured in the uterine mass and muscle for reader 1 were 343 mm^2 (range, 55–1631) and 157 mm^2 (range, 31–712), respectively, while those for reader 2 were 292 mm^2 (range, 55–1151) and 116 mm^2 (range, 25–404), respectively. Regarding the quantitative DWI-based parameters, both readers reported that the mean ADC value was lower in uterine sarcomas than in atypical leiomyomas, while the RCR was higher in uterine sarcomas than in atypical leiomyomas. For readers 1 and 2, the cutoff values for the mean ADC value and RCR were 1.05 x 10^{-3} mm^2/s and 4.76 and 0.87 x 10^{-3} mm^2/s and 5.65, respectively.

Diagnostic Classifier Development and Performance Analysis

Table 3 shows the results of the univariable and multivariable logistic regression analyses of qualitative MRI features in the training set. Univariable analysis revealed that irregular shape, ill-defined margins,

Table 1. Patient characteristics

Characteristic	Overall (n = 138)	ALM (n = 94)	US (n = 44)	*P*	Training (n = 84)	Validation (n = 54)	*P*
Age, yr	43.7 ± 10.3	40.3 ± 7.2	51.0 ± 12.2	< 0.001	44.1 ± 10.3	43.1 ± 10.4	0.763
Maximal diameter of tumor, mm	85.2 ± 41.3	81.3 ± 37.6	93.7 ± 47.8	0.238	85.4 ± 41.5	85.0 ± 41.5	> 0.999
Interval between MRI-surgery, day	41.2 ± 35.4	47.2 ± 36.1	28.4 ± 30.6	< 0.001	35.3 ± 28.8	50.4 ± 42.5	0.032
Initial surgery type				< 0.001			0.287
Hysterectomy	64 (46.4)	26 (27.7)	38 (86.4)		42 (50.0)	22 (40.7)	
Myomectomy	74 (53.6)	68 (72.3)	6 (13.6)		42 (50.0)	32 (59.3)	
Pathologic subtype				< 0.001			0.175
Leiomyoma	94 (68.1)	94 (100)	0 (0.0)		57 (67.9)	37 (68.6)	
Leiomyosarcoma	21 (15.2)	0 (0.0)	21 (47.7)		15 (17.9)	6 (11.1)	
Endometrial stromal sarcoma	19 (13.8)	0 (0.0)	19 (43.2)		8 (9.5)	11 (20.4)	
Adenosarcoma	1 (0.7)	0 (0.0)	1 (2.3)		1 (1.2)	0 (0.0)	
Undifferentiated sarcoma	1 (0.7)	0 (0.0)	1 (2.3)		1 (1.2)	0 (0.0)	
STUMP	2 (1.4)	0 (0.0)	2 (4.5)		2 (2.4)	0 (0.0)	
MRI scanner strength				0.494			0.589
1.5T	18 (13.0)	11 (11.7)	7 (15.9)		12 (14.3)	6 (11.1)	
3T	120 (87.0)	83 (88.3)	37 (84.1)		72 (85.7)	48 (88.9)	

Values are presented as patient number (%) or mean ± standard deviation.
ALM = atypical leiomyoma, US = uterine sarcoma, MRI = magnetic resonance imaging, STUMP = smooth muscle tumors of uncertain malignant potential

https://doi.org/10.3348/kjr.2023.0760

Korean Journal of Radiology
KJR

Table 2. Image analysis results of two readers

MRI features	Reader 1			Reader 2		
	ALM (n = 94)	US (n = 44)	*P*	ALM (n = 94)	US (n = 44)	*P*
Shape			< 0.001			< 0.001
Round/oval	58 (61.7)	12 (27.3)		65 (69.1)	16 (36.4)	
Irregular/lobulated	36 (38.3)	32 (72.7)		29 (30.9)	28 (63.6)	
Margin			< 0.001			0.078
Well-circumscribed	89 (94.7)	33 (75.0)		87 (92.6)	36 (81.8)	
Ill-defined	5 (5.3)	11 (25.0)		7 (7.4)	8 (18.2)	
Intratumoral hemorrhage			0.002			0.008
Absent	83 (88.3)	29 (65.9)		82 (87.2)	30 (68.2)	
Present	11 (11.7)	15 (34.1)		12 (12.8)	14 (31.8)	
T2 dark area			< 0.001			< 0.001
Present	66 (70.2)	11 (25.0)		78 (83.0)	10 (22.7)	
Absent	28 (29.8)	33 (75.0)		16 (17.0)	34 (77.3)	
Cystic areas on T2WI			0.022			0.143
Absent	62 (66.0)	20 (45.5)		73 (77.7)	29 (65.9)	
Present	32 (34.0)	24 (54.5)		21 (22.3)	15 (34.1)	
Central unenhanced area(s)			< 0.001			0.003
Absent	70 (74.5)	17 (38.6)		85 (90.4)	31 (70.5)	
Present	24 (25.5)	27 (61.4)		9 (9.6)	13 (29.5)	
ADC ($x10^{-3}$ mm^2/s)	1.24 ± 0.31	1.01 ± 0.30	< 0.001	1.23 ± 0.25	0.94 ± 0.30	< 0.001
RCR	4.13 ± 2.22	7.81 ± 4.85	< 0.001	4.19 ± 2.66	8.16 ± 2.94	< 0.001

Values are presented as patient number (%) or mean ± standard deviation.
MRI = magnetic resonance imaging, ALM = atypical leiomyoma, US = uterine sarcoma, T2WI = T2-weighted image, ADC = apparent diffusion coefficient, RCR = relative contrast ratio

Table 3. Univariable and multivariable logistic regression analysis of the qualitative MRI features in the training set

MRI features	Univariable analysis				Multivariable analysis	
	US	ALM	OR (95% CI)	*P*	aOR (95% CI)	*P*
Shape						
Round/oval	8 (29.6)	40 (70.2)	1 (reference)			
Irregular/lobulated	19 (70.4)	17 (29.8)	5.59 (2.12, 16.0)	< 0.001	3.16 (0.76, 14.2)	0.118
Margin						
Well-circumscribed	21 (77.8)	54 (94.7)	1 (reference)			
Ill-defined	6 (22.2)	3 (5.26)	5.14 (1.24, 26.2)	0.030	17.9 (1.41, 503)	0.040
Intratumoral hemorrhage						
Absent	16 (59.3)	50 (87.7)	1 (reference)			
Present	11 (40.7)	7 (12.3)	4.91 (1.66, 15.5)	0.005	27.3 (3.74, 596)	0.006
T2 dark area						
Present	6 (22.2)	48 (84.2)	1 (reference)			
Absent	21 (77.8)	9 (15.8)	18.7 (6.25, 64.1)	< 0.001	83.5 (12.4, 1916)	< 0.001
Cystic areas on T2WI						
Absent	18 (66.7)	41 (71.9)	1 (reference)			
Present	9 (33.3)	16 (28.1)	1.28 (0.47, 3.41)	0.623		
Central unenhanced area(s)						
Absent	19 (70.4)	54 (94.7)	1 (reference)			
Present	8 (29.6)	3 (5.26)	7.58 (1.97, 37.4)	0.005	6.10 (0.76, 76.5)	0.113

Values are presented patient number (%) unless otherwise indicated.
MRI = magnetic resonance imaging, US = uterine sarcoma, ALM = atypical leiomyoma, OR = odds ratio, CI = confidence interval, aOR = adjusted odds ratio, T2WI = T2-weighted image

https://doi.org/10.3348/kjr.2023.0760

intratumoral hemorrhage, absence of a T2 dark area, and central unenhanced area(s) were significantly associated with uterine sarcoma, but cystic areas in T2WI were not. In multivariable logistic regression analysis, ill-defined margins, intratumoral hemorrhage, and absence of T2 dark area were found to be significant independent MRI features that could differentiate uterine sarcoma from atypical leiomyoma. Diagnostic classifiers were constructed using the three qualitative MRI features as variables.

Tables 4, 5 and Figure 4 show the diagnostic performance metrics and ROC curves with AUC for the three classifiers. In the validation set, the logistic regression classifier using qualitative MRI features along with mean ADC values and RCR showed the highest performance, with an AUC of 0.92 (95% CI, 0.84–0.99), which was significantly higher than that of qualitative MRI features alone (AUC, 0.78; 95% CI, 0.65–0.91, $P < 0.001$).

Interobserver Agreement

Interobserver agreement for qualitative MRI features was fair to almost perfect; shape ($\kappa = 0.35$), margin ($\kappa = 0.67$), intratumoral hemorrhage ($\kappa = 0.86$), absence of T2 dark area ($\kappa = 0.60$), cystic areas in T2WI ($\kappa = 0.33$), and central irregular non-enhancing area(s) ($\kappa = 0.35$). The reproducibility of the quantitative parameters was substantial (ICC, 0.68; 95% CI, 0.58–0.76 for the mean ADC value and ICC, 0.72; 95% CI, 0.63–0.79 for the RCR). A detailed description of the interobserver agreement is provided in Supplementary Table 2.

DISCUSSION

We explored six established qualitative MRI features recognized as indicative of uterine sarcoma and identified three statistically significant independent differentiating features in our study group: ill-defined margins, intratumoral hemorrhage, and absence of T2 dark areas. The inclusion of DWI-based quantitative parameters improved the diagnostic performance of logistic regression classifiers in distinguishing uterine sarcomas from atypical leiomyomas in both the training and validation sets. Furthermore, the addition of quantitative parameters significantly mitigated the performance decline observed in the validation set, suggesting an improved generalizability of the classifier.

Our study included a relatively large number of patients with uterine sarcomas evaluated to date to differentiate uterine sarcomas from atypical leiomyomas using qualitative and quantitative MRI features. The outcomes of this investigation can be regarded as a sequence of external validations that corroborate the results of previous studies.

Table 4. Comparison of the AUC between three classifiers in the training and validation sets

	AUC in training set	*P*	AUC in validation set	*P*
Classifier				
Qualitative	0.90 (0.84, 0.97)		0.78 (0.65, 0.91)	
Qualitative + ADC	0.93 (0.87, 0.99)	0.094	0.85 (0.74, 0.96)	0.027
Qualitative + ADC + RCR	0.94 (0.88, 1.00)	0.073	0.92 (0.84, 0.99)	< 0.001

Numbers are raw data, and numbers in parentheses are 95% confidence intervals.
'Qualitative,' 'Qualitative + ADC,' and 'Qualitative + ADC + RCR' includes selected qualitative MRI features alone, selected qualitative MRI features + ADC value, and selected qualitative MRI features + ADC value + RCR, respectively. The *P*-value is compared with selected qualitative MRI features alone.
AUC = area under the receiver operating characteristic curve, ADC = apparent diffusion coefficient, RCR = relative contrast ratio, MRI = magnetic resonance imaging

Table 5. Comparison of the diagnostic performance between three classifiers in the validation set

	Qualitative	Qualitative + ADC	Qualitative + ADC + RCR
Metrics			
Accuracy	0.80 [43/54] (0.66, 0.89)	0.83 [45/54] (0.71, 0.92)	0.87 [47/54] (0.75, 0.95)
Sensitivity	0.76 [13/17] (0.56, 0.97)	0.88 [15/17] (0.73, 1.00)	0.88 [15/17] (0.73, 1.00)
Specificity	0.81 [30/37] (0.68, 0.94)	0.81 [30/37] (0.68, 0.94)	0.86 [32/37] (0.75, 0.98)

Numbers in brackets are raw data, and numbers in parentheses are 95% confidence intervals.
'Qualitative,' 'Qualitative + ADC,' and 'Qualitative + ADC + RCR' includes selected qualitative MRI features alone, selected qualitative MRI features + ADC value, and selected qualitative MRI features + ADC value + RCR, respectively. The cutoff point of logistic classifiers was determined by ROC curve with maximum Youden index in the training set.
ADC = apparent diffusion coefficient, RCR = relative contrast ratio, ROC = receiver operating characteristic, MRI = magnetic resonance imaging

https://doi.org/10.3348/kjr.2023.0760

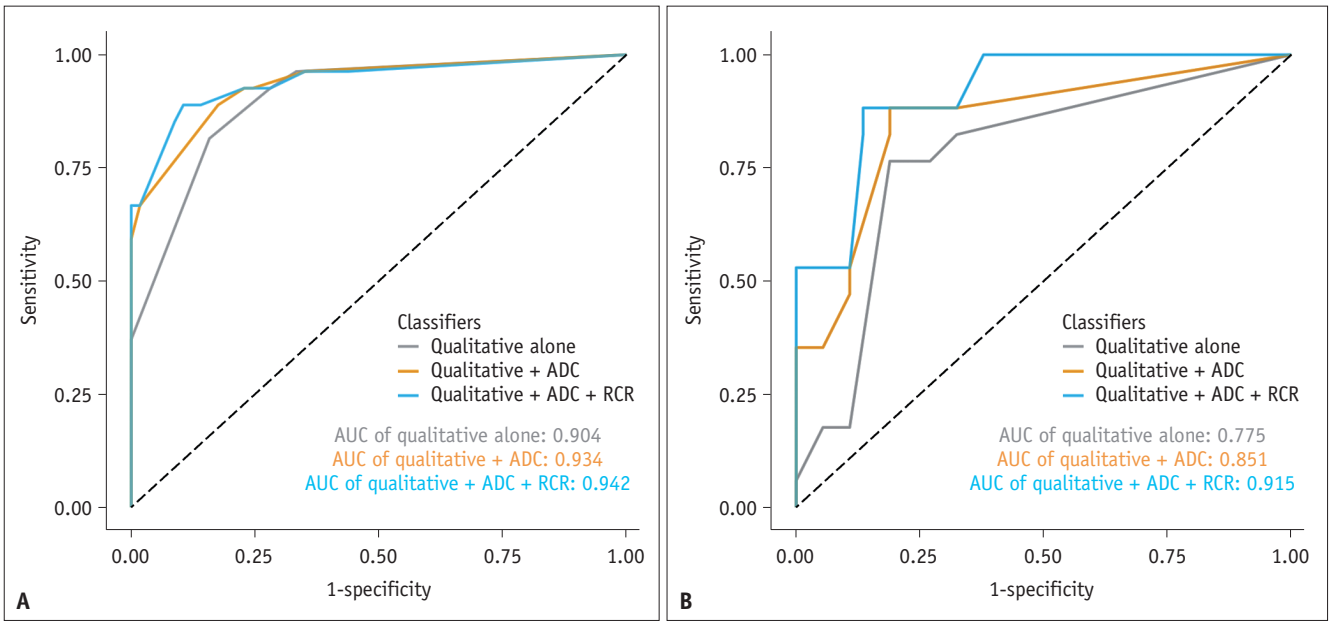

Fig. 4. AUC-ROC curves of three logistic regression classifiers in the training set **(A)** and validation set **(B)**. AUC-ROC = area under the receiver operating characteristic curve, ADC = apparent diffusion coefficient, RCR = relative contrast ratio

The qualitative MRI features previously documented to favor uterine sarcoma are irregular shape [12,29], ill-defined margins [12,18,30], intratumoral hemorrhage [12], absence of a T2 dark area [11], heterogeneous SI in T2WI [17], heterogeneous contrast enhancement [17,18], and central irregular non-enhancing area(s) [12,22]. Hyperintensity of mass in DWI was a significant feature of uterine sarcoma in some studies [17,18,23]. This study verified the qualitative MRI features suggested in previous studies and obtained relatively consistent results within our dataset. In particular, our multivariable logistic regression analysis revealed that ill-defined margins, intratumoral hemorrhage, and the absence of T2 dark area were significant independent MRI features, while irregular shapes and central irregular non-enhancing areas(s) were not. This discrepancy may be attributed to variations in the inclusion of different types and numbers of uterine sarcomas across the studies. Populations across various studies exhibited heterogeneity, including studies that included carcinosarcomas, those focused exclusively on leiomyosarcomas, and those considering typical and atypical leiomyomas. Another factor contributing to these discrepancies is the ambiguity in defining qualitative MRI features. For example, the "T2 dark signal area" has been used with various interpretations in different studies. Some research groups have used it to describe the non-enhancing hemorrhagic component, indicating malignancy [12], while others have used it to enhance solid tissues, suggesting benign characteristics [11]. In our study, the presence of a T2 dark signal area was considered a typical finding in uterine leiomyomas, and we adopted the concept of the "absence of a T2 dark signal area" as an indicator of malignancy. It is reasonable to anticipate significant progress in resolving these discrepancies in the future, since a consensus has recently been made on the lexicon of qualitative MRI features that are important for distinguishing uterine sarcoma [31].

In a previous study, only cases with a single mass were included, and it was reported that 71.8% of single masses in patients aged ≥ 44.8 years were malignant [17]. However, in our study, 65.9% (29/44) of uterine sarcomas presented as solitary masses, while 41.5% (39/94) of atypical leiomyomas presented as single masses. Another recent study indicated that 51% of sarcomas were found among multiple masses [26]. Therefore, determining the potential presence or absence of uterine sarcomas based solely on the number of lesions should be avoided.

Although many studies have reported consistent key qualitative MRI features of uterine sarcomas, they remain highly subjective, resulting in variable interobserver agreement. The accurate interpretation of these findings requires sufficient clinical experience. In contrast, ADC values have been shown to be consistent quantitative parameters for improving the diagnostic ability to differentiate uterine sarcomas from atypical leiomyomas, and the usefulness

 https://doi.org/10.3348/kjr.2023.0760

of the ADC value has been previously demonstrated in the literature [11-15,17,19,22,23,26,29,30]. In a recent consensus publication [31], a comprehensive analysis of ADC cutoff values from various previous studies has been performed and the reported range of the cutoff values was found to be 0.91–1.29 x 10^{-3} mm^2/s. In our study, the ADC value cutoff was 1.05 x 10^{-3} mm^2/s for reader 1 and 0.87 x 10^{-3} mm^2/s for reader 2. In particular, the ADC cutoff value for reader 2 was the lowest among the values reported to date. However, the ADC values pose several challenges. For example, even in benign leiomyoma, the fibrotic component may exhibit prominent T2 dark SI, leading to a very low ADC value, which is known as the "T2 blackout effect." Furthermore, the ADC value may be influenced by variations in magnetic field strength in different MRI scanners and manufacturers [32,33]. Therefore, in this study, we used the RCR as a parameter to address the inherent challenges related to the ADC values. The RCR serves as a normalized quantitative parameter designed to rectify the limitations associated with the ADC values. A similar approach was previously applied to T2WI to quantify the SI of the tumor, represented as tumor-myometrium contrast ratio, using the following formula: $(SI_{tumor} - SI_{myometrium})/SI_{myometrium}$ [14]. However, we believe that normalized values, such as RCR, are more necessary and useful than those obtained from T2WI owing to the intrinsic vulnerability of DWI acquisition.

Our study has several limitations. First, this was a retrospective study and selection bias could not be completely avoided. Second, different subtypes of uterine sarcomas that might exhibit distinct imaging features were grouped into a single category. Most of the cases were leiomyosarcomas and ESS, and rare subtypes, such as smooth uterine muscles with uncertain malignant potential or undifferentiated sarcomas, were rarely included. However, leiomyosarcoma and ESS did not show significant differences in imaging features in our study (Supplementary Table 3), and we believe that the infrequent occurrence of other rare subtypes may not have significantly affected the overall results. Moreover, in clinical practice, differentiation between leiomyomas and uterine sarcomas is more important than distinguishing between the various subtypes of uterine sarcoma. Third, MRI acquisition parameters and scanner manufacturers were relatively heterogeneous because this study included patients from several different institutions to collect as many cases of uterine sarcoma as possible. However, it should be noted that a considerable number of cases were scanned using the same equipment and that there were no major differences in protocols between the different equipment. Consequently, we expected that the potential effects of heterogeneity on the overall results would be limited. Fourth, external validation of the logistic regression classifier is not feasible. Although the addition of quantitative parameters exhibited robust generalization performance in the internal validation set, it will be imperative for future studies to confirm these outcomes using external validation sets. Finally, we obtained the ADC value and the RCR by manually delineating ROIs in the area of the ADC map with the most restricted diffusion; however, this step cannot avoid certain levels of interobserver and intraobserver variability.

In conclusion, DWI-based quantitative parameters, including the mean ADC value and RCR, have an additional value when added to qualitative MRI features, as they improve diagnostic performance in differentiating uterine sarcoma from atypical leiomyoma. These parameters can be easily measured in clinical practice.

Supplement

The Supplement is available with this article at https://doi.org/10.3348/kjr.2023.0760.

Availability of Data and Material

The datasets generated or analyzed during the study are not publicly available due to personal information protection act but are available from the corresponding author on reasonable request.

Conflicts of Interest

The authors have no potential conflicts of interest to disclose.

Author Contributions

Conceptualization: Sung Eun Rha. Data curation: Hokun Kim, Sung Eun Rha. Formal analysis: Hokun Kim, Sung Eun Rha, Eu Hyun Kim, Ahwon Lee. Investigation: Hokun Kim, Eu Hyun Kim, Yu Ri Shin, Soo Youn Park, Su-Lim Lee, Mee-Ran Kim. Methodology: Sung Eun Rha, Hokun Kim. Project administration: Sung Eun Rha. Resources: Hokun Kim, Eu Hyun Kim, Sung Eun Rha. Software: Hokun Kim. Supervision: Sung Eun Rha. Validation: Hokun Kim, Sung Eun Rha. Visualization: Hokun Kim, Sung Eun Rha. Writing—original draft: Hokun Kim, Eu Hyun Kim, Sung Eun Rha. Writing—review & editing: Hokun Kim, Sung Eun Rha, Yu Ri Shin.

ORCID IDs
Hokun Kim
https://orcid.org/0000-0003-0884-7946
Sung Eun Rha
https://orcid.org/0000-0003-1514-929X
Yu Ri Shin
https://orcid.org/0000-0001-5695-4426
Eu Hyun Kim
https://orcid.org/0000-0003-0061-649X
Soo Youn Park
https://orcid.org/0009-0001-0874-611X
Su-Lim Lee
https://orcid.org/0000-0001-7109-353X
Ahwon Lee
https://orcid.org/0000-0002-2523-9531
Mee-Ran Kim
https://orcid.org/0000-0003-4492-0768

Funding Statement
None

REFERENCES

1. Stewart EA. Uterine fibroids. *Lancet* 2001;357:293-298
2. Wallach EE, Vlahos NF. Uterine myomas: an overview of development, clinical features, and management. *Obstet Gynecol* 2004;104:393-406
3. Ryan GL, Syrop CH, Van Voorhis BJ. Role, epidemiology, and natural history of benign uterine mass lesions. *Clin Obstet Gynecol* 2005;48:312-324
4. Amant F, Coosemans A, Debiec-Rychter M, Timmerman D, Vergote I. Clinical management of uterine sarcomas. *Lancet Oncol* 2009;10:1188-1198
5. Mallmann P. Uterine sarcoma - difficult to diagnose, hard to treat. *Oncol Res Treat* 2018;41:674
6. Mbatani N, Olawaiye AB, Prat J. Uterine sarcomas. *Int J Gynaecol Obstet* 2018;143 Suppl 2:51-58
7. Major FJ, Blessing JA, Silverberg SG, Morrow CP, Creasman WT, Currie JL, et al. Prognostic factors in early-stage uterine sarcoma. A Gynecologic Oncology Group study. *Cancer* 1993;71(4 Suppl):1702-1709
8. Yorgancı A, Meydanlı MM, Kadıoğlu N, Taşkın S, Kayıkçıoğlu F, Altın D, et al. Incidence and outcome of occult uterine sarcoma: a multi-centre study of 18604 operations performed for presumed uterine leiomyoma. *J Gynecol Obstet Hum Reprod* 2020;49:101631
9. Hricak H, Tscholakoff D, Heinrichs L, Fisher MR, Dooms GC, Reinhold C, et al. Uterine leiomyomas: correlation of MR, histopathologic findings, and symptoms. *Radiology* 1986;158:385-391
10. Murase E, Siegelman ES, Outwater EK, Perez-Jaffe LA, Tureck RW. Uterine leiomyomas: histopathologic features, MR imaging findings, differential diagnosis, and treatment. *Radiographics* 1999;19:1179-1197
11. Abdel Wahab C, Jannot AS, Bonaffini PA, Bourillon C, Cornou C, Lefrère-Belda MA, et al. Diagnostic algorithm to differentiate benign atypical leiomyomas from malignant uterine sarcomas with diffusion-weighted MRI. *Radiology* 2020;297:361-371
12. Lakhman Y, Veeraraghavan H, Chaim J, Feier D, Goldman DA, Moskowitz CS, et al. Differentiation of uterine leiomyosarcoma from atypical leiomyoma: diagnostic accuracy of qualitative MR imaging features and feasibility of texture analysis. *Eur Radiol* 2017;27:2903-2915
13. Tamai K, Koyama T, Saga T, Morisawa N, Fujimoto K, Mikami Y, et al. The utility of diffusion-weighted MR imaging for differentiating uterine sarcomas from benign leiomyomas. *Eur Radiol* 2008;18:723-730
14. Namimoto T, Yamashita Y, Awai K, Nakaura T, Yanaga Y, Hirai T, et al. Combined use of T2-weighted and diffusion-weighted 3-T MR imaging for differentiating uterine sarcomas from benign leiomyomas. *Eur Radiol* 2009;19:2756-2764
15. Takeuchi M, Matsuzaki K, Nishitani H. Hyperintense uterine myometrial masses on T2-weighted magnetic resonance imaging: differentiation with diffusion-weighted magnetic resonance imaging. *J Comput Assist Tomogr* 2009;33:834-837
16. Cornfeld D, Israel G, Martel M, Weinreb J, Schwartz P, McCarthy S. MRI appearance of mesenchymal tumors of the uterus. *Eur J Radiol* 2010;74:241-249
17. Thomassin-Naggara I, Dechoux S, Bonneau C, Morel A, Rouzier R, Carette MF, et al. How to differentiate benign from malignant myometrial tumours using MR imaging. *Eur Radiol* 2013;23:2306-2314
18. Bonneau C, Thomassin-Naggara I, Dechoux S, Cortez A, Darai E, Rouzier R. Value of ultrasonography and magnetic resonance imaging for the characterization of uterine mesenchymal tumors. *Acta Obstet Gynecol Scand* 2014;93:261-268
19. Sato K, Yuasa N, Fujita M, Fukushima Y. Clinical application of diffusion-weighted imaging for preoperative differentiation between uterine leiomyoma and leiomyosarcoma. *Am J Obstet Gynecol* 2014;210:368.e1-e8
20. Zhang GF, Zhang H, Tian XM, Zhang H. Magnetic resonance and diffusion-weighted imaging in categorization of uterine sarcomas: correlation with pathological findings. *Clin Imaging* 2014;38:836-844
21. Tasaki A, Asatani MO, Umezu H, Kashima K, Enomoto T, Yoshimura N, et al. Differential diagnosis of uterine smooth muscle tumors using diffusion-weighted imaging: correlations with the apparent diffusion coefficient and cell density. *Abdom Imaging* 2015;40:1742-1752
22. Lin G, Yang LY, Huang YT, Ng KK, Ng SH, Ueng SH, et al. Comparison of the diagnostic accuracy of contrast-enhanced MRI and diffusion-weighted MRI in the differentiation between uterine leiomyosarcoma/smooth muscle tumor with uncertain malignant potential and benign leiomyoma. *J Magn Reson*

Imaging 2016;43:333-342
23. Li HM, Liu J, Qiang JW, Zhang H, Zhang GF, Ma F. Diffusion-weighted imaging for differentiating uterine leiomyosarcoma from degenerated leiomyoma. *J Comput Assist Tomogr* 2017;41:599-606
24. Kim TH, Kim JW, Kim SY, Kim SH, Cho JY. What MRI features suspect malignant pure mesenchymal uterine tumors rather than uterine leiomyoma with cystic degeneration? *J Gynecol Oncol* 2018;29:e26
25. Valdes-Devesa V, Jimenez MDM, Sanz-Rosa D, Espada Vaquero M, Alvarez Moreno E, Sainz de la Cuesta Abbad R. Preoperative diagnosis of atypical pelvic leiomyoma and sarcoma: the potential role of diffusion-weighted imaging. *J Obstet Gynaecol* 2019;39:98-104
26. Xie H, Zhang X, Ma S, Liu Y, Wang X. Preoperative differentiation of uterine sarcoma from leiomyoma: comparison of three models based on different segmentation volumes using radiomics. *Mol Imaging Biol* 2019;21:1157-1164
27. Jagannathan JP, Steiner A, Bay C, Eisenhauer E, Muto MG, George S, et al. Differentiating leiomyosarcoma from leiomyoma: in support of an MR imaging predictive scoring system. *Abdom Radiol (NY)* 2021;46:4927-4935
28. Ogihara Y, Kitazume Y, Iwasa Y, Taura S, Himeno Y, Kimura T, et al. Prediction of histological grade of hepatocellular carcinoma using quantitative diffusion-weighted MRI: a retrospective multivendor study. *Br J Radiol* 2018;91:20170728
29. Hélage S, Vandeventer S, Buy JN, Bordonné C, Just PA, Jacob D, et al. Uterine sarcomas: are there MRI signs predictive of histopathological diagnosis? A 50-patient case series with pathological correlation. *Sarcoma* 2021;2021:8880080
30. Barral M, Placé V, Dautry R, Bendavid S, Cornelis F, Foucher R, et al. Magnetic resonance imaging features of uterine sarcoma and mimickers. *Abdom Radiol (NY)* 2017;42:1762-1772
31. Hindman N, Kang S, Fournier L, Lakhman Y, Nougaret S, Reinhold C, et al. MRI evaluation of uterine masses for risk of leiomyosarcoma: a consensus statement. *Radiology* 2023;306:e211658
32. Zhu J, Zhang J, Gao JY, Li JN, Yang DW, Chen M, et al. Apparent diffusion coefficient normalization of normal liver: will it improve the reproducibility of diffusion-weighted imaging at different MR scanners as a new biomarker? *Medicine (Baltimore)* 2017;96:e5910
33. Schmeel FC. Variability in quantitative diffusion-weighted MR imaging (DWI) across different scanners and imaging sites: is there a potential consensus that can help reducing the limits of expected bias? *Eur Radiol* 2019;29:2243-2245

https://doi.org/10.3348/kjr.2023.0760